Surface Chemistry

International Edition: DOI: 10.1002/anie.201609317
German Edition: DOI: 10.1002/ange.201609317

Growth of Stable Surface Oxides on Pt(111) at Near-Ambient Pressures

Donato Fantauzzi[+], Sandra Krick Calderón[+], Jonathan E. Mueller, Mathias Grabau, Christian Papp, Hans-Peter Steinrück, Thomas P. Senftle, Adri C. T. van Duin, and Timo Jacob**

Abstract: *Detailed knowledge of the structure and degree of oxidation of platinum surfaces under operando conditions is essential for understanding catalytic performance. However, experimental investigations of platinum surface oxides have been hampered by technical limitations, preventing in situ investigations at relevant pressures. As a result, the time-dependent evolution of oxide formation has only received superficial treatment. In addition, the amorphous structures of many surface oxides have hindered realistic theoretical studies. Using near-ambient pressure X-ray photoelectron spectroscopy (NAP-XPS) we show that a time scale of hours ($t \geq 4$ h) is required for the formation of platinum surface oxides. These experimental observations are consistent with ReaxFF grand canonical Monte Carlo (ReaxFF-GCMC) calculations, predicting the structures and coverages of stable, amorphous surface oxides at temperatures between 430–680 K and an O_2 partial pressure of 1 mbar.*

The widespread use of platinum in heterogeneous catalysis and electrochemistry runs the gamut from model systems to industrial applications,[1,2] making platinum surfaces the object of extensive study. Surface oxide formation is a key challenge in understanding their catalytic properties since many of the catalyzed reactions are carried out in oxygen-rich environments. Indeed, surface oxidation is reported to alter the catalytic activity and selectivity of platinum.[3,4] Recent atomistic simulations[5] elucidated the surface oxidation of Pt(111) for coverages up to $\Theta_O \leq 1$ ML, predicting structures and energetics consistent with scanning tunneling microscopy and temperature-programmed desorption (TPD) experiments.[6] The initial stages of surface oxidation are attributed to surface buckling and subsurface oxygen, resulting from processes that are both accessible at low temperatures.[5] Similar behavior has been observed in the presence of H_2O.[7] At $\Theta_O \geq 1.25$ ML, experiments indicated the formation of "oxidic" oxygen on Pt(111), leading to the formation of PtO_x particles, followed by kinetically limited growth of a disordered oxide film with $\Theta_O = 2.4$ ML[8] and $\Theta_O = 2.9$ ML.[9] Due to the large unit cells required to reliably model amorphous surface oxides, density functional theory (DFT) calculations have only been applied to highly ordered surface oxide structures.[10]

Recently surface science techniques, conventionally limited to ultrahigh vacuum (UHV) conditions, have been applied to investigate systems at near-ambient pressures (NAP),[11–14] making quantitative observation of adsorbates and surface oxidation states possible in situ. Such NAP experiments circumvent the transfer of the system from elevated pressures to UHV conditions during which the catalyst surface is often altered.[15,16] Miller et al. used NAP-XPS to study platinum surface oxides in situ[17] without examining their temporal evolution. Zhu et al. investigated the early stages of surface oxide formation on stepped Pt(557) using high-pressure scanning tunneling microscopy and NAP-XPS to characterize the nucleation and growth of platinum oxide clusters as a function of the O_2 partial pressure.[18] Both studies extract a shift in the Pt 4f levels from their XPS data for diverse surface oxides in the range of 1.1–1.6 eV to higher binding energies.

To quantitatively investigate the growth and structure of high-coverage oxygen surface phases on Pt(111), we performed in situ NAP-XPS measurements at O_2 partial pressures of 1 mbar and temperatures between 300 and 700 K. ReaxFF-GCMC[19] calculations were used to rationalize the experimental findings and to identify and characterize the stabilities of amorphous surface oxide structures.

To investigate the growth of platinum oxide at various temperatures, the O 1s and Pt 4f regions were monitored in situ during extended exposure to 1 mbar of O_2. Figure 1a

[*] Dr. D. Fantauzzi,[+] Dr. J. E. Mueller, Prof. Dr. T. Jacob
Institute of Electrochemistry, Ulm University
Albert-Einstein-Allee 47, 89069 Ulm (Germany)
and
Helmholtz Institute Ulm (HIU) Electrochemical Energy Storage
89081 Ulm (Germany)
and
Karlsruhe Institute of Technology (KIT)
P.O. Box 3640, 76021 Karlsruhe (Germany)
E-mail: timo.jacob@uni-ulm.de

S. Krick Calderón,[+] M. Grabau, Dr. C. Papp, Prof. Dr. H.-P. Steinrück
Lehrstuhl für Physikalische Chemie II
Universität Erlangen-Nürnberg
Egerlandstr. 3, 91058 Erlangen (Germany)
E-mail: christian.papp@fau.de

Dr. T. P. Senftle
Department of Mechanical and Aereospace Engineering
Princeton University
Princeton, NJ 08544-5263 (USA)

Prof. Dr. A. C. T. van Duin
Department of Mechanical and Nuclear Engineering
Pennsylvania State University
University Park, PA 16801 (USA)

[+] These authors contributed equally to this work.

Supporting information for this article, including a method section describing the NAP-XPS and ReaxFF-GCMC approach and details of the measurements and calculations, can be found under: http://dx.doi.org/10.1002/anie.201609317.

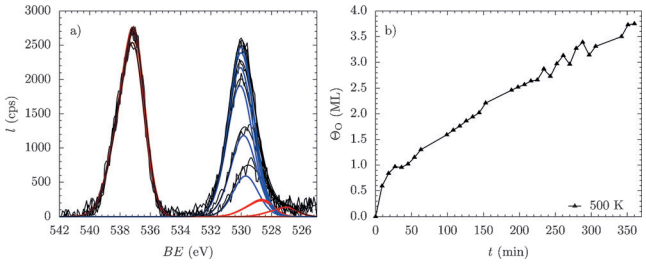

Figure 1. a) Selected O 1s spectra for the growth at $p(O_2) = 1$ mbar and a sample temperature of 500 K. Gas-phase (red) and surface components (blue) and b) the respective growth curve obtained by deconvolution of the surface signal.

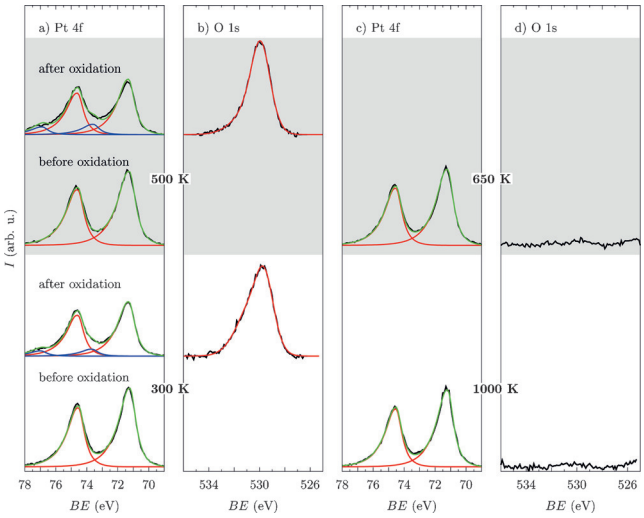

Figure 2. a) Pt 4f spectra before (lower) and after (upper) an oxidation experiment at $p(O_2) = 1$ mbar at 300 and 500 K. b) O 1s spectra after the experiments with a coverage of 3.7 and 3.8 ML, respectively. Saturation was reached after 300 and 360 minutes for the growth at 300 and 500 K, respectively. c) Pt 4f spectra after heating the sample to 1000 and 650 K, respectively, and d) the corresponding O 1s spectra.

shows selected in situ O 1s spectra during the oxidation of Pt(111) at 1 mbar of O_2 and a sample temperature of 500 K. The O_2 gas phase emerges at 537.2 eV with its X-ray satellites at 527.1 and 528.7 eV (red fit) and the surface species at 529.7 eV (blue fit). The quantitative analysis of this experiment is shown in Figure 1 b. Within the time resolution of our experiment, a coverage exceeding 0.5 ML is reached quickly followed by steady growth, which continues for at least the duration of the experiment (360 minutes). The O 1s spectra for similar experiments carried out at 300, 400, 600, 650, and 700 K are shown in Figure S1 in the Supporting Information. At the end of the oxidation experiments, platinum oxide coverages of 3.7 ML (300 K), 1.9 ML (400 K), 3.8 ML (500 K), 1.5 ML (600 K), 0.5 ML (650 K), and 0.3 ML (700 K) were obtained. The high sensitivity of these experiments to trace impurities in the crystal (e.g. Si, Ca, etc.[20–22]) and residual gas (e.g. CO, hydrocarbons etc.) makes reproduction of exact surface coverages at defined time scales difficult. As the formed oxides are not stable in UHV at temperatures above 400 K, they were cooled in 1 mbar O_2 ($T < 350$ K) before pump-down to UHV conditions.

Pt 4f and O 1s spectra taken in UHV before and after oxidation are shown in Figures 2 a and b, respectively. In addition to the metallic Pt $4f_{7/2}$ and $4f_{5/2}$ contributions at 71.3 and 74.6 eV, the spectra taken after oxidation at 300 and 500 K contain contributions at 73.7 and 77.0 eV (corresponding to a 2.4 eV higher binding energy), which can be attributed to platinum oxide.[17] A closer inspection of the O 1s spectra points to differences in these two surface oxides, even though they both correspond to an oxygen coverage of about 3.7 ML. For 300 K the maximum is found at 529.7 eV, whereas for 500 K it is shifted by 0.2 eV towards higher binding energies to 529.9 eV and the peak is more symmetric, indicating an additional oxygen species at 300 K. Heating the oxides grown at 300 and 500 K to 1000 and 650 K (under UHV conditions), respectively, cleans the surface and returns Pt to the metallic state as can be seen in Figures 2 c and d. Note that the minor intensity in the O 1s region results from the adsorption of residual gases. In contrast to previous investigations, where oxide formation was not detected below 400 K,[17,23] we observe pronounced oxide growth at 300 K. Our longer exposure times compared with other published experiments[4,17] may explain this difference, suggesting that the growth of platinum oxide is diffusion-limited due to kinetic hindrances previously discussed in the literature.[9]

While XPS provided time-dependent quantitative information on the chemical state of the surface, atomistic simulations can be used to shed light on their structures and obtain a deeper understanding of the chemical processes occurring at higher chemical potentials. To systematically investigate high-coverage surface oxide formation, ReaxFF-GCMC simulations were carried out corresponding to the experimental conditions.

Each simulation started with a clean 9 layer Pt(111) slab, both sides of which were available for oxidation. Results from the simulations are provided in the Supporting Information. (Meta)stable surface oxide structures, which were used to construct the phase diagram shown in Figure 3, were identified at two simulation temperatures, namely 600 and 650 K (see Figures S6 b and S7 b). The phase diagram predicts the existence of stable amorphous surface oxides for oxygen chemical potentials in the range of $-1.01\,\text{eV} \leq \Delta\mu_O \geq -0.64\,\text{eV}$ (corresponding to 430–680 K at 1 mbar O_2, area C in Figure 3), and five stable surface phases for increasing oxygen chemical potential: A clean Pt(111), B $p(2\times2)$ adsorbed atomic oxygen, C a low- and a high-coverage surface oxide phase (1 and 2) and D α-PtO_2 bulk oxide.

Surface oxide growth curves from NAP-XPS measurements and GCMC simulations are shown in Figures 4 a and b, respectively. By taking the final experimental coverages as points of reference the MC iteration scales are converted to time scales in Figure 4 c, even providing predictions of the behavior of the experimental growth curves for longer exposure times. The simulated growth curves at 400, 600, and 650 K show additional increases in surface coverage from 1.5 to 3.5 ML, 1.1 to 3.5 ML, and 0.5 to 1.0 ML, respectively,

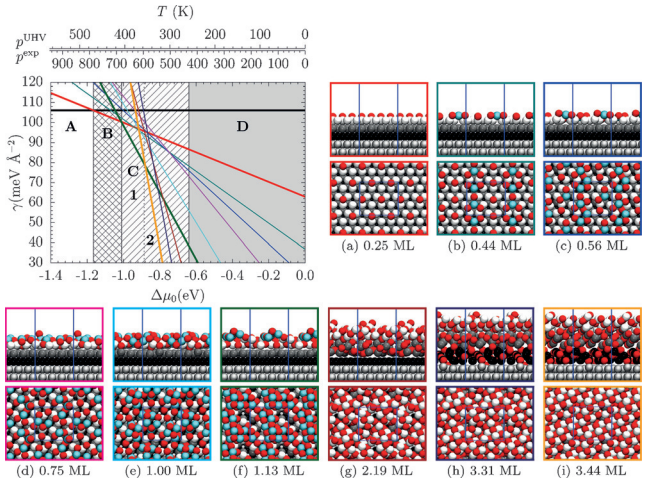

Figure 3. Phase diagram for Pt(111) surface oxidation derived from low-energy structures obtained in ReaxFF-GCMC simulations at a MC temperature of 650 and 600 K. Temperature scales in degrees Kelvin for values of $\Delta\mu_O$ at oxygen partial pressures $p(O_2)$ corresponding to UHV (10^{-10} mbar) and experimental (1 mbar) conditions are given at the very top. Side and top views of the most stable and metastable structures (a)–(i) with their respective surface unit cells are shown in boxes, the colors of which correspond to the color of the relevant phase line in the phase diagram. Oxygen atoms are red; platinum atoms are various shades of gray, depending on which layer they belong to in the initial structure or light blue when buckled (only for $\Theta_O \leq 1.13$ ML). The phase diagram shows five thermodynamically stable phases: A clean Pt(111), B $p(2\times2)$ adsorbed atomic oxygen, C a low- and a high-coverage surface oxide phases (1 and 2) and D α-PtO_2 bulk oxide.

during the simulation "time" (i.e. iterations) extending beyond the duration of the experiments (see arrows in Figure 4c). The final coverages of the experimentally grown oxides are summarized in Figure 5 together with the simulated stability range of each phase. Consistent with our simulated phase diagram (see UHV scale in Figure 3), the oxygen phases grown at 600, 650, and 700 K were not stable under UHV and had to be determined from the final in situ spectra, leading to an error in the coverage determination of up to 20%. Considering this margin of error, the 0.3 ML obtained by XPS at 700 K agrees with the 0.25 ML coverage predicted by the simulated phase diagram (area B in Figure 5). At 650 K our simulated phase diagram predicts that a surface oxide with a coverage of 1.13 ML is stable (area C1 in Figure 5). Therefore, we predict that additional exposure time is required for forming this structure experimentally. At 600 K, a coverage of 1.5 ML was obtained in the NAP-XPS experiment, while the coverage in the GCMC simulation plateaus at 1 ML before further oxidation leads to a second plateau at 3.5 ML. To probe the possibility of further oxide growth at 600 K, we prepared a 1.1 ML oxide at 300 K and then heated it in situ to 600 K, leading to further oxide growth in the following 200 minutes of the experiment (see Figure S3). The need for this jumpstart in order to form high-coverage surface oxides within the time scale of our experiment (400 minutes) at 600 K is consistent with the slow growth rate observed in the GCMC simulation at this temperature. Alternatively, these kinetics might be due to the disproportionate influence of surface defects, which play a key role in nucleating platinum oxide clusters, as has been demonstrated on stepped platinum surfaces.[18] Because 600 K lies at the transition between low-coverage (1.13 ML) and high-coverage (3.44 ML) surface oxide phases (area C1 and C2 in Figure 5), minor fluctuations in the experimental temperature or tiny differences in the calculated surface free energies may determine which side of this boundary the system lies on. At temperatures between 600 and 430 K our phase diagram predicts a 3.44 ML surface oxide (area C2 in Figure 5), which becomes metastable below 430 K (area D in Figure 5). In line with this prediction, we obtained the highest experimental coverages in measurements at 300 and 500 K, in which we observed additional features in the Pt 4f core level at 2.4 eV higher binding energies consistent with the formation of platinum oxide, further supporting the GCMC simulations. At 400 K the steady growth up to 2.0 and 3.5 ML observed experimentally and in the GCMC simulations, respectively, is expected to proceed to bulk oxide formation in accordance with the surface phase diagram. The slower growth kinetics and resulting lower coverage observed at 400 K, compared with 300 and 500 K, may reflect the strong influence of contaminates (e.g. hydrocarbons) below the detection limit. Alternatively enhanced diffusion in the crystal at 500 K may explain the slower growth kinetics at 400 K, in the face of a stronger driving force.

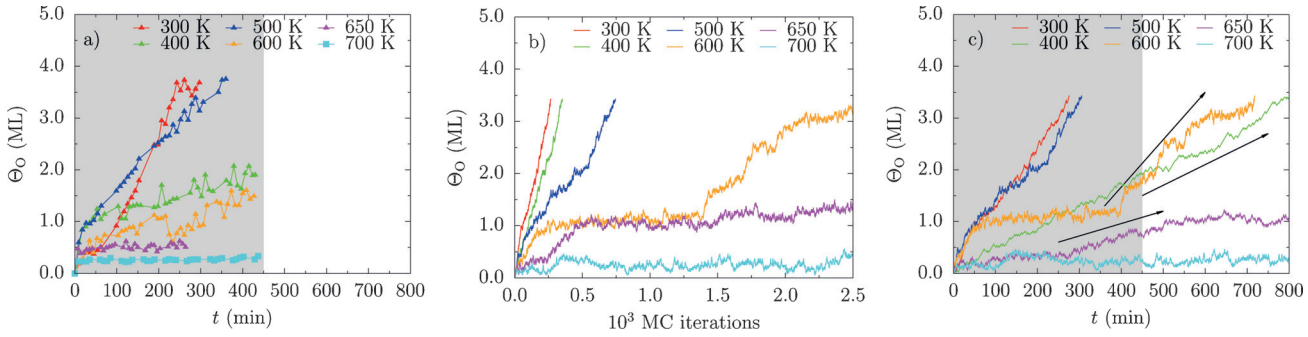

Figure 4. Results for platinum oxide growth at $p(O_2) = 1$ mbar and different temperatures obtained from a) experiments and ReaxFF-GCMC simulations b) before and c) after calibrating the MC iterations for each temperature to the respective experimental time scale of the growth curve. Arrows in (c) indicate theoretical predictions of further oxide growth for longer exposure times.

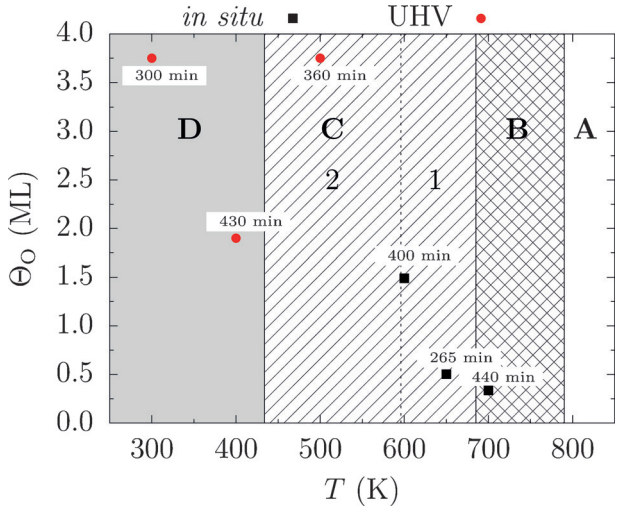

Figure 5. Experimental coverages of the platinum oxides grown at different temperatures and $p(O_2) = 1$ mbar obtained from in situ O 1s spectra (black squares) and UHV spectra after pump-down (red circles) are shown along with the theoretically predicted stability range of the different phases: A clean Pt(111), B $p(2\times2)$ adsorbed atomic oxygen, C a low- and a high-coverage surface oxide phases (1 and 2) and D α-PtO_2 bulk oxide.

The relationship between the surface oxides reported here and the ozone-derived oxide reported elsewhere[8] could be experimentally explored by comparing NAP-XPS synchrotron measurements. Calculated Pt 4f levels for a model step-edge oxide, exhibiting a PtO_2-motif predominant in α- and β-PtO_2 bulk oxides and closely mimicked by our amorphous surface oxides, resulted in a shift of 1.3 eV to higher binding energies (see Figure S10), corresponding nicely to (synchrotron) NAP-XPS experiments on stepped Pt(557) that found a shift of 1.1 eV.[18]

In conclusion, the oxidation of a Pt(111) surface exposed to O_2 was investigated using NAP-XPS and ReaxFF-GCMC simulations. Extended time scales ($t \leq 4$ h) were critical for forming the thermodynamically stable platinum surface oxides experimentally, that our ReaxFF-GCMC simulations predict to be stable at 1 mbar of O_2 and temperatures between 430 and 680 K. The shorter exposure times used in other published experiments explains their failure to observe these stable surface oxides.[17] The stability window of the surface oxides lies between a bulk oxide phase at lower chemical potentials ($T < 430$ K, $p(O_2) = 1$ mbar) and an adsorbed-oxygen phase at higher chemical potentials ($T > 680$ K, $p(O_2) = 1$ mbar). Stable surface oxides have major implications for Pt-based (electro-)catalysis and in particular for catalytic conditions within their thermodynamic stability window, since their catalytic properties may differ dramatically from those of bare platinum.

Acknowledgements

S.K.C., M.G., C.P., and H.P.S. greatly acknowledge support by the Cluster of Excellence Engineering of Advanced Materials (EAM) at the Friedrich-Alexander-University Erlangen-Nürnberg. D.F., J.E.M., and T.J. thank the financial support from the DFG (Deutsche Forschungsgemeinschaft) and the European Research Council through the ERC-StartingGrant THEOFUN (grant agreement number 259608). J.E.M. gratefully acknowledges support from the Alexander von Humboldt Foundation. T.P.S. and A.C.T.v.D. acknowledge funding from the National Science Foundation grants CBET-1032979 and CHE-1505607. The authors thank Dr. Josef Anton for fully-relativistic all-electron calculations on the core-level shifts. The authors also acknowledge the computer time supported by the state of Baden-Württemberg through the bwHPC project and the DFG through grant number INST40/467-1 FUGG.

Conflict of interest

The authors declare no conflict of interest.

Keywords: interfaces · kinetics · oxidation · phase transitions · surface chemistry

How to cite: *Angew. Chem. Int. Ed.* **2017**, *56*, 2594–2598
Angew. Chem. **2017**, *129*, 2638–2642

[1] P. N. Ross, *Handbook of Fuel Cells: Fundamentals, Technology, Applications*, Wiley-VCH, Weinheim, **2003**, pp. 465–480.
[2] T. Engel, G. Ertl, *Advances in Catalysis*, Academic Press, New York, **1979**, pp. 1–78.
[3] C. E. Smith, J. P. Biberian, G. A. Somorjai, *J. Catal.* **1979**, *57*, 426–443.
[4] D. Miller, H. Sanchez Casalongue, H. Bluhm, H. Ogasawara, A. Nilsson, S. Kaya, *J. Am. Chem. Soc.* **2014**, *136*, 6340–6347.
[5] D. Fantauzzi, J. E. Mueller, L. Sabo, A. C. T. v. Duin, T. Jacob, *ChemPhysChem* **2015**, *16*, 2797–2802.
[6] S. P. Devarajan, J. A. Hinojosa, Jr., J. F. Weaver, *Surf. Sci.* **2008**, *602*, 3116–3124.
[7] M. J. Eslamibidgoli, M. H. Eikerling, *Electrocatalysis* **2016**, *7*, 345–354.
[8] N. A. Saliba, Y. L. Tsai, C. Panja, B. E. Koel, *Surf. Sci.* **1999**, *419*, 79–88.
[9] J. F. Weaver, J.-J. Chen, A. L. Gerrard, *Surf. Sci.* **2005**, *592*, 83–103.
[10] N. Seriani, W. Pompe, L. C. Ciacchi, *J. Phys. Chem. B* **2006**, *110*, 14860–14869.
[11] H. Bluhm, M. Hävecker, A. Knop-Gericke, M. Kiskinova, R. Schlögl, M. Salmeron, *MRS Bull.* **2007**, *32*, 1022–1030.
[12] D. E. Starr, Z. Liu, M. Hävecker, A. Knop-Gericke, H. Bluhm, *Chem. Soc. Rev.* **2013**, *42*, 5833–5857.
[13] M. Salmeron, R. Schlögel, *Surf. Sci. Rep.* **2008**, *63*, 169–199.
[14] F. Tao, M. Salmeron, *Science* **2011**, *331*, 171–174.
[15] M. D. Ackermann, T. M. Pedersen, B. L. M. Hendriksen, O. Robach, S. C. Bobaru, I. Popa, C. Quiros, H. Kim, B. Hammer, S. Ferrer, J. W. M. Frenken, *Phys. Rev. Lett.* **2005**, *95*, 255505.
[16] F. Tao, S. Dag, L.-W. Wang, Z. Liu, D. R. Butcher, H. Bluhm, M. Salmeron, G. A. Somorjai, *Science* **2010**, *327*, 850–853.
[17] D. J. Miller, H. Öberg, S. Kaya, H. Sanchez Casalongue, D. Friebel, T. Anniyev, H. Ogasawara, H. Bluhm, L. G. M. Pettersson, A. Nilsson, *Phys. Rev. Lett.* **2011**, *107*, 195502.
[18] Z. Zhu, F. Tao, F. Zheng, R. Chang, Y. Li, L. Heinke, Z. Liu, M. Salmeron, G. A. Somorjai, *Nano Lett.* **2012**, *12*, 1491–1497.
[19] T. P. Senftle, R. J. Meyer, M. J. Janik, A. C. T. van Duin, *J. Chem. Phys.* **2013**, *139*, 044109.

[20] H. Niehus, G. Comsa, *Surf. Sci. Lett.* **1981**, *102*, L14 – L20.
[21] M. Salmerón, L. Brewer, G. A. Somorjai, *Surf. Sci.* **1981**, *112*, 207 – 228.
[22] H. Bonzel, A. Franken, G. Pirug, *Surf. Sci.* **1981**, *104*, 625 – 642.
[23] A. Farkas, K. Zalewska-Wierzbicka, C. Bachmann, J. Goritzka, D. Langsdorf, O. Balmes, J. Janek, H. Over, *J. Phys. Chem. C* **2013**, *117*, 9932 – 9942.

Manuscript received: September 22, 2016
Revised: December 12, 2017
Final Article published: January 25, 2017

